INTERNATIONAL JOURNAL OF OPTIMIZATION IN CIVIL ENGINEERING
Int. J. Optim. Civil Eng., 2018; 8(3):381-399

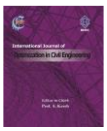

PREDICTION OF BIAXIAL BENDING BEHAVIOR OF STEEL-CONCRETE COMPOSITE BEAM-COLUMNS BY ARTIFICIAL NEURAL NETWORK

A. Behnam and M. R. Esfahani[*, †]
Department of Civil Engineering, Faculty of Engineering, Ferdowsi University of Mashhad, Iran

ABSTRACT

In this study, the complex behavior of steel encased reinforced concrete (SRC) composite beam–columns in biaxial bending is predicted by multilayer perceptron neural network. For this purpose, the previously proposed nonlinear analysis model, mixed beam-column formulation, is verified with biaxial bending test results. Then a large set of benchmark frames is provided and P-M_x-M_y triaxial interaction curve is obtained for them. The specifications of these frames and their analytical results are defined as inputs and targets of artificial neural network and a relatively accurate estimation model of the nonlinear behavior of these beam-columns is presented. In the end, the results of neural network are compared to some analytical examples of biaxial bending to determine the accuracy of the model.

Keywords: steel-concrete composite; composite beam-column; steel encased reinforced concrete; nonlinear analysis; artificial neural network; multilayer perceptron.

Received: 10 September 2017; Accepted: 12 November 2017

1. INTRODUCTION

SRC steel-concrete composite frames are highly efficient and economic structures that directed less attention than concrete and steel structures due to the complexities in their behavior analysis. The features of steel structures include high strength, ductility and fast implementation. Also concrete structures are cost effective and durable and have high resistance to fire. Composite structures by using steel and concrete in the appropriate location, utilize the features of both groups. SRC columns include higher resistance to

[*]Corresponding author: Department of Civil Engineering, Faculty of Engineering, Ferdowsi University of Mashhad, Iran
esfahani@um.ac.ir (M. R. Esfahani)

reinforced concrete columns in the same section, resistance against fire and corrosion of steel, more unbraced length in tall columns and more resistance against explosion and strike.

Different models are presented for analyzing the behavior of composite beam-columns. Three types of modeling are possible for these structures. The first model is a continuous three-dimensional analysis which is very accurate. In this analysis, concrete and steel are modeled with brick and shell elements and contact surface of two materials are modeled with gap and frictional elements. Schneider [1], Johansson and Gylltoft [2],Varma et al. [3], Hu et al. [4] used this model to analyze composite beam-columns. Despite high accuracy, heavy cost of calculations makes this method impractical in analysis of frames. The second model considers the nonlinear behavior of material only at the end of the members' joints and it is called concentrated plasticity model. Hajjar and Gourley [5], El-Tawil and Deierlein [6], Inai et al. [7] used this model to examine the behavior of composite beam-columns. The third model is distributed plasticity model which provides nonlinear behavior of materials at integration points of member elements. This method has higher accuracy compared to concentrated plasticity. Also it requires less time to analyze than a continuous three-dimensional model. Hajjar et al. [8], Aval et al. [9], Varma et al. [3], Tort et al. [10], Denavit and Hajjar [11], Liang et al. [12] and Denavit et al. [13] have used distributed plasticity model to analyze composite beam-columns. Among these models Denavit and Hajjar [11], Liang et al. [12] have used three-dimensional model for biaxial bending analysis of these beam-columns.

Many different experiments have been conducted with regard to investigation of behavior and biaxial bending resistance of composite beam–columns. Virdi and Dowling [14] tested ultimate strength of SRC beam-columns in biaxial bending. In these experiments, 9 concrete beam-column samples with central core in the form of H in biaxial eccentricity and lengths were examined. In 1984, Morino et al. [15] conducted laboratory studies on elasto-plastic behavior of SRC composite beam-columns by applying biaxial eccentricity loading. In these experiments, eccentricity effects, the angle between the loading point and the main axis and slenderness ratio on load-displacement behavior and maximum load capacity were performed. Munoz and Hsu [16] applied curvilinear axial force and biaxial bending on four small scale concrete beam-columns with I-shaped steel core. The sections include one short column and three slender columns with square sections.

Different types of artificial neural networks have been used in various civil engineering subjects, including estimation of beam–columns behavior. These networks with nonlinear behavior and large number of parameters are able to accurately estimate different issues. Kaveh and Iranmanesh [17-19] performed a comparative study of backpropagation and improved counter propagation neural networks in structural analysis and optimization. Ahmadi et al. [20, 21] predicted the capacity of short and long circular composite columns filled with concrete under axial load. The input data are laboratory results and the effects of yield stress, tube wall thickness, column length, concrete strength and column dimensions have been investigated. Kaveh et al. [22, 23] predicted the moment-rotation characteristic for saddle-like and semi-rigid connections using FEM and BP neural networks. Afaq et al. [24] examined the effect of steel fibers on load bearing capacity of RC beams using artificial neural network. The database of neural networks has been extracted from previous results of experiments and after validation, this network was used for a parametric research on the effect of various parameters related to steel fibers, material properties, and cross sectional

geometry. By analyzing output estimates, it was determined that this neural network can quantify the effects of different parameters for RC load capacity. Kaveh and Servati [25, 26] used artificial neural networks for the purpose of analysis and design optimization of double layer grids. Also Kaveh and Raiessi Dehkordi [27] investigated the application of artificial neural networks in predicting the deformation of domes under wind load. Kumar and Yadav [28] performed beam–columns buckling analysis using mathematical model and neural network of multilayer perceptron, and compared the output results of neural network with Euler's mathematical formula. Rofoei et al. [29] estimated the vulnerability of the concrete moment resisting frame structures using artificial neural networks. Kotsovou et al. [30] predicted the behavior of circumferential RC beam–columns connections using neural network. The neural network predictions for failure mode and load bearing capacity of these connections confirmed the shortcomings in the regulation which was previously identified by analytical methods. Sadowski et al. [31] performed and compared non-destructive detection of adhesion tension of a concrete substrate layer added to concrete layer with variable thickness using a neural network and with different algorithms.

There are only a few experiments on biaxial bending of composite beam–columns which are limited to axial forces and specific angles. Therefore, it is not possible to create a neural network using laboratory results to predict their behavior. Also due to complexity and time-consuming analytical methods, it is not possible to easily use them for researchers. For this reason, in this study after re-verification of composite columns model of Denavit and Hajjar [32] with the laboratory results of biaxial bending, a large set of square SRC composite columns with different lengths and dimensions created and for each one the three dimensional P-M_x-M_y interaction curve was designed. After that, by using multilayer perceptron neural network, a fairly accurate estimate for three-dimensional behavior of these columns was presented and the neural network output was compared with analytical results to determine the accuracy of model.

2. NONLINEAR ANALYSIS

2.1 Constitutive relationships presented for composite sections

Nonlinear behavior of material in cross section is followed at integral points within the element. The cycling comprehensive constitutive formulas for steel and concrete presented in the researches of Denavit and Hajjar [32] have been used. These models consider prominent features of each material and the interaction between them.

Constitutive formulas between concrete and steel are selected in accordance with AISC 360-16 [33] and ACI 318-14 [34] regulations. Therefore, in this study, the tension in concrete has been neglected and local buckling has not been considered. The method based on Chang and Mander [35] is used for the cyclic behavior of concrete. Also for uniform response of concrete strength Popovic equation [36] (equation 1) has been used. A schematic view of this relationship is presented in Fig. 1. The confined model of Mander [37] has been used to determine the increase of compressive strength and ductility.

Popovic (1973)

$$y = \frac{rx}{r - 1 + x^r} \tag{1a}$$

$$r = \frac{n}{n - 1} \tag{1b}$$

In these formulas, x is normalized strain and n is normalized module of elasticity.

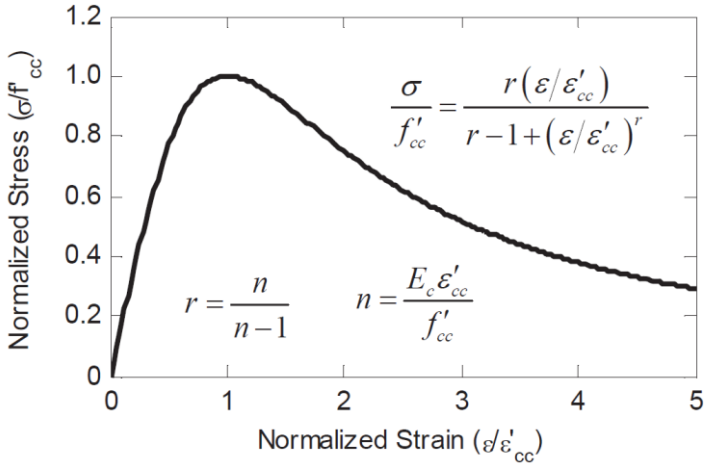

Figure 1. Constitutive formula presented by Popovic for uniform response of concrete

In SRC columns, constitutive formula of elastic–perfectly plastic has been used to model the steel core. This formula is defined with initial stiffness and yield strength (Fig. 2). This model is suitable to be used in hot-rolled steel sections and armatures.

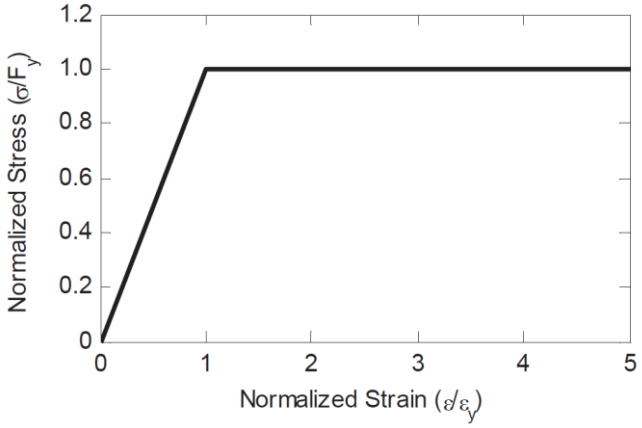

Figure 2. elastic–perfectly plastic constitutive relationship for steel sections of SRC beam-columns

The members are modeled as fiber sections which present the structural behavior of each part of section. In SRC sections, concrete is considered to be highly confined between flanges of steel section. In this area, confining pressure is provided by steel section and lateral armatures. El-Tawil and Deierlein [6] presented a mechanism in which confined

pressure created by steel section is calculated by equation 2a, only along the y axis, by considering plastic moment capacity of the flange, shown in Fig. 5a. The distance between parabolic vertex and central line of steel section is defined with equation 2b. This area indicates the boundary between highly confined area and medium confined area. This parabolic area has been modeled in different directions of the steel section directly with different equations (Fig. 3b). The area between cover and parabolic shape is modeled in order to provide average behavior through using *ke* coefficient.

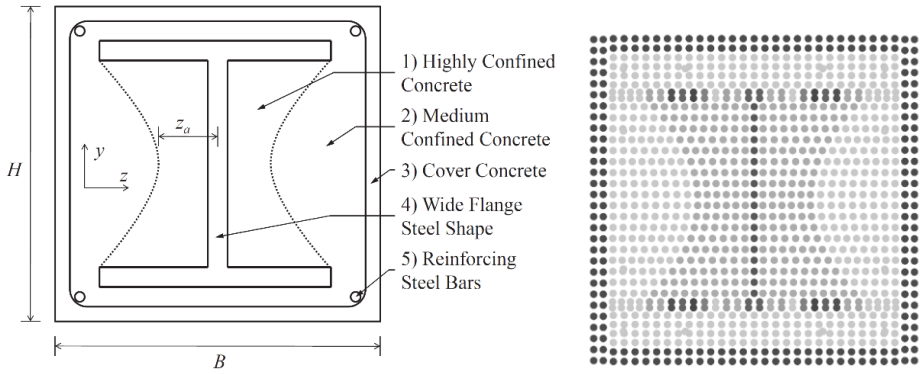

(a) (b)

Figure 3. SRC fiber cross section (a) Different area division of SRC column section, (b) A sample of fiber section of SRC composite column

$$F_{ly,high} = F_{ly,medium} + \frac{t_f^2 F_{ys}}{0.75(b_f - t_w)^2} \tag{2a}$$

$$z_a = 0.50b_f - 0.25(d - 2t_f) \geq 0.50t_w \tag{2b}$$

$$r_{n,post} = 0.75 \tag{2c}$$

2.1 The formulation used in nonlinear analysis

Beam elements are classified based on major unknown variables into three groups including displacement-based, force-based and the mixture of these two methods. In the deformation-based method, or in other words stiffness method, elements consider joint deformations as major unknowns, Hajjar and Gourley [5], Aval et al. [9], Alemdar and White [38].

The deformations of element are calculated using interpolator functions. The equilibrium of the element is satisfied only in a variational state and internal forces of element do not accurately satisfy the equilibrium. This type of formulation is normally considered for use and expansion of simple nonlinear geometric behavior. Interpolator functions, which are commonly used for deformations, only model linear curvature distribution along the element. This is a very important limitation, especially when the plastic joints are formed which causes a highly nonlinear curvature distribution. In force-based method, or in other words softness method, the elements consider tensions as the major unknowns, De Souza [39], El-Tawil and Deierlein [6], Alemdar and White [38].

The forces are calculated along the length of elements using interpolator functions. The equilibrium of the element is certainly satisfied but compatibility of deformations in element

will be only satisfied in the variational state. Compared to element with displacement-based method, force-based elements are often time-consuming and have high computational costs. Elements mixed by element forces and joint displacements are considered as the major unknowns which allows the use of interpolator functions for deformation of elements and stresses along with the length of element, Nukala and White [40], Alemdar and White [38], Tort and Hajjar [10], Denavit and Hajjar [11].

Despite complexity of analysis process, which is usually longer than the methods based on displacement and force, the mixed method is a proper balance between estimation of nonlinear curves along the element and the ability to consider direct nonlinear geometric behavior.

In this study, mixed beam element, implemented in the framework of OpenSees software by Denavit and Hajjar [11, 32] has been used for the nonlinear analysis of composite columns.

2.2 Interaction curve

By a set of complete nonlinear analysis, interaction curves of biaxial bending moment – axial forces for each section and each frame was created. An analysis was performed only with axial force to determine the critical axial load, then a set of analysis was carried out to apply constant axial load and incremental lateral load. In the case of zero axial load, section analysis was performed instead of frame analysis. In each analysis, the critical point is determined when the minimum eigenvalue is zero. In cases where this does not occur, the critical point is created when the maximum longitudinal strain in each section of each member reaches 0.05. At critical point, the amount of applied loads and internal forces is recorded, and it is possible to construct the interaction curve of first-order loads and interaction of second-order internal forces. A sample of these diagrams is shown for SRC sections and a frame in Fig. 4.

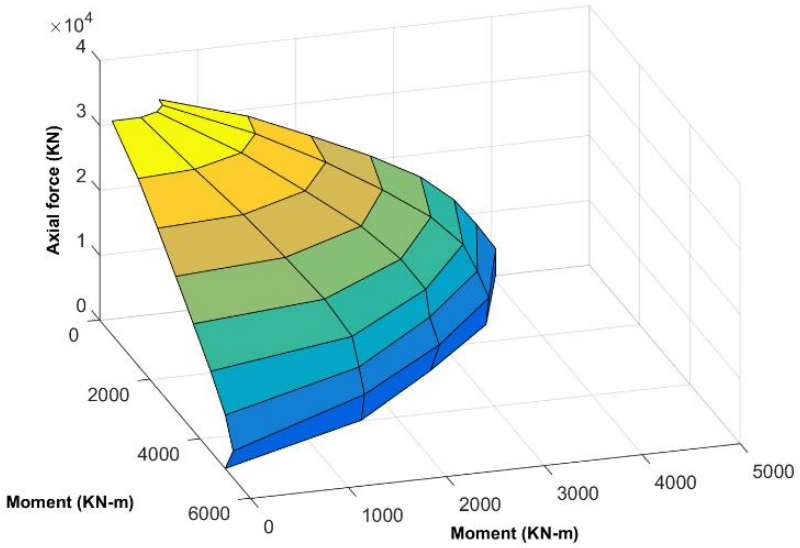

Figure 4. P-M_x-M_y triaxial interaction curve for SRC-BBB-4 composite beam-column

3. COMPARING THE MODEL WITH BIAXIAL LABORATORY RESULTS

The nonlinear model described in the previous section is compared and verified in Denavit and Hajjar [32] research with the existing laboratory results. In this section, the results of nonlinear analysis of SRC columns with biaxial bending tests are verified by Morino et al. [15] and Virdi and Dowling [14]. That is, P-M_x-M_y interaction diagram for the sections used in the tests is obtained by using nonlinear analysis. Because in tests the biaxial bending behavior is examined only in one axial load, three-dimensional interaction curve was cut at this axial load and Mx-My two-dimensional curve was obtained. In this case, the recorded moments in the lab was compared with analysis results. In table 3 the ratio of test results to analysis results is presented. Fig. 4 is an example of this comparison.

Table 1 shows the specifications of concrete sections in tested SRC columns. These specifications include concrete strength, yield strength of the longitudinal and transverse armatures, columns dimensions, diameter of bars, the reinforcement spacing and concrete cover. Table 2 shows the specifications of steel sections used in SRC columns including steel yield strength, web and flange dimensions and their thickness. In table 3 the ratio of analysis results to test results is presented for these columns. The average ratio of analysis moment to test moment for these 13 samples is 1.0 and standard deviation is 0.08. The results clearly show the strong performance of nonlinear analysis. Figs. 5a and 5b show the M_x-M_y two-dimensional interaction diagram for samples A4-60 and H in axial loads of 524.89 KN (118 kip) and 355.86 KN (80 kip). It should be noted that the naming of samples is based on a reference article.

Table 1: The specifications of concrete section dimensions and materials of SRC composite columns

Spec.	H(mm)	B(mm)	f_c(MPa)	d_b(mm)	Fylr(MPa)	d_{bTies}(mm)	s(mm)	F_{ytr}(MPa)	cover(mm)
A4-60	160.02	160.02	21.10	6.35	413.70	4.06	150.11	413.70	19.05
A8-45	160.02	160.02	33.58	6.35	413.70	4.06	150.11	413.70	19.05
B4-45	160.02	160.02	23.37	6.35	413.70	4.06	150.11	413.70	19.05
B4-60	160.02	160.02	23.37	6.35	413.70	4.06	150.11	413.70	19.05
B8-45	160.02	160.02	33.30	6.35	413.70	4.06	150.11	413.70	19.05
B8-60	160.02	160.02	33.30	6.35	413.70	4.06	150.11	413.70	19.05
C8-45	160.02	160.02	24.62	6.35	413.70	4.06	150.11	413.70	19.05
C8-60	160.02	160.02	24.62	6.35	413.70	4.06	150.11	413.70	19.05
D4-45	160.02	160.02	21.24	6.35	413.70	4.06	150.11	413.70	19.05
D8-45	160.02	160.02	22.89	6.35	413.70	4.06	150.11	413.70	19.05
D8-60	160.02	160.02	22.89	6.35	413.70	4.06	150.11	413.70	19.05
H	254.00	254.00	39.72	12.70	308.69	4.83	152.40	308.69	25.40
I	254.00	254.00	43.16	12.70	308.69	4.83	152.40	308.69	25.40

Table 2: The specifications of steel section dimensions of SRC composite columns

Spec.	d(mm)	t_w(mm)	b_f(mm)	t_f(mm)	F_y (MPa)
A4-60	100.08	6.10	100.08	7.87	344.75
A8-45	100.08	6.10	100.08	7.87	344.75
B4-45	100.08	6.10	100.08	7.87	344.75
B4-60	100.08	6.10	100.08	7.87	344.75
B8-45	100.08	6.10	100.08	7.87	344.75
B8-60	100.08	6.10	100.08	7.87	344.75
C8-45	100.08	6.10	100.08	7.87	344.75
C8-60	100.08	6.10	100.08	7.87	344.75
D4-45	100.08	6.10	100.08	7.87	344.75
D8-45	100.08	6.10	100.08	7.87	344.75
D8-60	100.08	6.10	100.08	7.87	344.75
H	152.40	6.35	152.40	6.35	314.69
I	152.40	6.35	152.40	6.35	314.69

Table 3: The ratio of test results to nonlinear analysis results for SRC columns

Spec.	H(mm)	B(mm)	L(mm)	Angle	P_{exp} (KN)	M_{exp} (KN.m)	M_{anal}(KN.m)	M_{anal}/M_{exp}	Ref.
A4-60	160.02	160.02	960.12	60.00	524.02	24.15	24.42	1.01	Morino 1984
A8-45	160.02	160.02	960.12	45.00	378.61	31.63	30.07	0.95	Morino 1984
B4-45	160.02	160.02	2400.30	45.00	389.60	23.43	23.69	1.01	Morino 1984
B4-60	160.02	160.02	2400.30	60.00	436.39	26.99	24.38	0.90	Morino 1984
B8-45	160.02	160.02	2400.30	45.00	294.19	31.27	29.22	0.93	Morino 1984
B8-60	160.02	160.02	2400.30	60.00	328.31	33.28	31.24	0.94	Morino 1984
C8-45	160.02	160.02	3600.45	45.00	195.27	25.88	24.37	0.94	Morino 1984
C8-60	160.02	160.02	3600.45	60.00	194.02	23.04	26.61	1.15	Morino 1984
D4-45	160.02	160.02	4800.60	45.00	209.01	19.10	18.12	0.95	Morino 1984
D8-45	160.02	160.02	4800.60	45.00	146.61	21.69	22.67	1.04	Morino 1984
D8-60	160.02	160.02	4800.60	60.00	158.35	21.29	24.25	1.14	Morino 1984
H	254.00	254.00	7432.29	30.11	353.66	84.20	86.90	1.03	Virdi 1973
I	254.00	254.00	7432.29	30.11	293.88	96.38	89.74	0.93	Virdi 1973
							Mean	1.00	
							Standard Deviation	0.08	
							Coheficient of Variation	0.08	

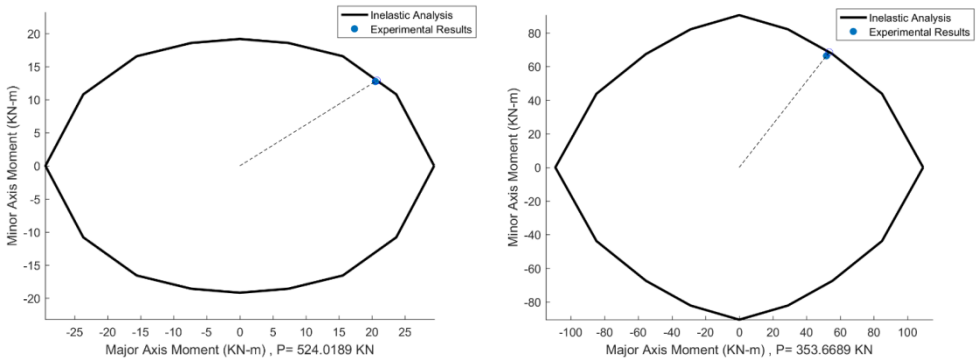

(a) (b)

Figure 5. M_x-M_y two-dimensional interaction curve: (a) A4-60 specimen, (b) H specimen

4. BENCHMARK FRAMES

In researches of Kanchanalai [41], Surovek-Maleck and White [42, 43], benchmark frames with supporting conditions and various lateral bracings were used to analyze the stability of steel columns. Denavit et al. [13] expanded these frames and used with a set of composite sections of CFT and SRC to analyze the stability of composite columns. One of the main features of these base frames is the complete coverage of possible modes for composite beam – columns in terms of supporting conditions, lateral bracings, column bearing loads, material strength and the size of sections. In this study, these SRC composite sections and frames have been used to obtain a complete set of interaction curves of biaxial bending moment – axial force related to composite columns in different situations.

4.1 Sections

SRC composite section are selected to incorporate practical range of concrete strength and steel ratio. Other specifications of sections such as steel yield stress are considered to be common values. Steel yield stress for rectangular sections of wide flange W is considered to be Fy = 344.74MPa (50 ksi). For concrete with a typical strength f'c = 27.6MPa (4 ksi) and for high strength concrete it is f'c = 68.9MPa (10 ksi).

In composite section there is no upper limit for steel ratio. But practical and dimensional considerations in which the steel sections are made will impose the upper limit of about 12% for SRC. Also AISC 360-16 regulation considers at least 1% steel for composite sections. Also this design code specified minimum of 0.4% for reinforcement and there is no specification for maximum value. ACI regulation specified maximum of 8% for reinforcement.

Given these limitations, three wide flange section of W for SRC section, three reinforcement configuration and three external dimensions of 560 mm in 560 mm (22 in 22 inches), 710 mm in 710 mm (28 in 28 inches), and 865 mm in 865 mm (34 in 34 inches) have been used. A total of 36 sections (18 sections and two concrete strengths) were selected for SRCs. Table 4 and 5 show the type and ratio of used steel and the configuration of SRC sections reinforcement.

Table 4: Selected steel sections

Index	Steel Shape	ρ_s
A	W360x463	11.66%
B	W360x347	8.74%
C	W360x179	4.49%
SRC steel shapes		

Table 5: Reinforcement configuration

Index	Steel Shape	ρ_s
A	20 #36	3.98%
B	12 #32	1.94%
SRC reinforcing configuration		

The agreement for naming the sections is three parts which are separated by a dash. These parts include SRC section type, section shape and concrete strength. For example, the SRC-ACB-4 considers SRC which is made of a section with external dimension of 560 mm in 560 mm, a steel section of W360x179, 12 # 32 reinforcement and a concrete with strength of f'c = 27.6 MPa. These sections are shown schematically in Fig. 6.

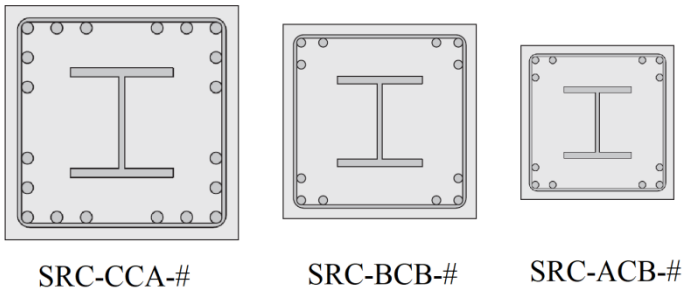

Figure 6. The schematic design of sections in different dimensions

4.2 Frames

Denavit et al. [13] expanded the benchmark frames used in the previous researches and utilized them to analyze the stability of composite columns. In this research the three-dimensional model of these frames was used to analyze the behavior of SRC composite columns in biaxial bending. This set include sidesway-inhibited frames and various end conditions. Frames have been expanded and their parameters for three-dimensional behavior of composite sections have been developed. This frame is shown schematically in Fig. 7.

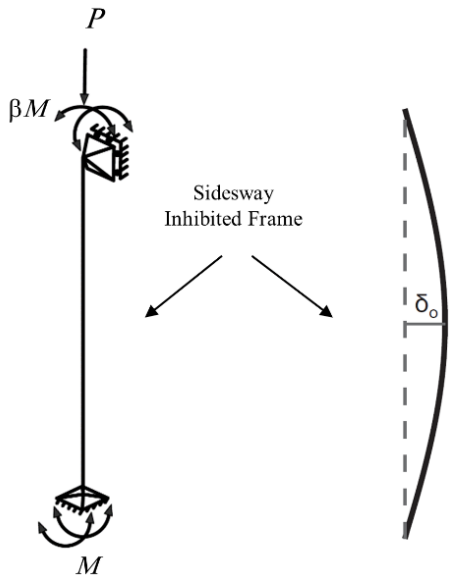

(a) Composite Beam-Column (b) Initial geometric imperfection

Figure 7. Schematic view of benchmark frame

Sidesway-inhibited frames are defined with slenderness coefficient of λ_{oe1g} and the end moments ratio of β. With λ_{oe1g}, length of each frame (L) is calculated using equation 3. In this equation, $EI_{g(w)}$ is gross elastic rigidity of weak axis and P_{nog} is nominal zero-length compressive strength. The value of these parameters for selected framed is presented in Table 6.

Table 6: The variables of base frames

Frame	Slenderness	End moment ratio	Number of frames
Sidesway-inhibited	4 values $\lambda oe1g$ =0.45,0.90,1.35,1.90	4 values β=0,1,2,3	16

4.3 Initial geometric imperfection

Numerical geometric imperfections equal to the manufacturing and installation tolerances in AISC 360-16 were explicitly modeled. For all frames out-of-straightness was considered the half sine wave with a maximum range of L/1000 (Fig. 7b).

5. DATA ACQUISITION TO BE USED IN ARTIFICIAL NEURAL NETWORK

In this section the obtained results in the inelastic analysis part of benchmark frames are classified to be used in artificial neural networks. In this study, the results of sidesway-inhibited frame analysis have been used for training the neural network. The number of samples is 576 frames.

In order to define each frame, 10 variables including *L* length of the element, *B* cross section width, b_f steel section width, t_f flange thickness of steel section, t_w web thickness of steel section, *d* depth of steel section, *db* diameter of armatures, *No.* number of armatures, f'_c concrete strength and β bending coefficient were used. Since steel yield strength is considered the same for all framed F_y was removed from the inputs. The input data of neural network for frames with lateral bracing is presented in Table 7.

The target output of neural network are P-M_x-M_y interaction curves for each frame which are not symmetric due to steel shape used. So, with the angles of 0, 22.5, 45, 67.5 and 90 degrees, we can design interaction curve. In each angle, there are 7 values of moments for each component of x and y. by finding the sum of square roots of M_x and M_y for each group, a value of M is obtained. Therefore, there will be a total of 35 moments for five angles. Also to reflect the value of axial force, the maximum Pmax is sufficient. Because this value is divided into equal intervals from Pmax to zero. Accordingly, the interaction curve in each frame can be described.

According to what we already said, the modeled neural network for composite columns has 10 inputs and 36 outputs and 576 samples.

Table 7: Input data of neural network for frames with lateral bracing

Number of Frames	Length (mm)	B(mm)	ϭ	d(mm)	t_w(mm)	b_f(mm)	t_f(mm)	F'_c(MPa)	db(mm)	rebar No.
1	5967.48	558.80	-0.5	434.34	35.81	411.48	57.40	27.58	35.81	20
2	7240.52	711.20	-0.5	434.34	35.81	411.48	57.40	27.58	35.81	20
3	8820.15	863.60	-0.5	434.34	35.81	411.48	57.40	27.58	35.81	20
4	5621.78	558.80	-0.5	434.34	35.81	411.48	57.40	68.95	35.81	20
5	6750.56	711.20	-0.5	434.34	35.81	411.48	57.40	68.95	35.81	20
6	8090.66	863.60	-0.5	434.34	35.81	411.48	57.40	68.95	35.81	20
7	6107.43	558.80	-0.5	434.34	35.81	411.48	57.40	27.58	32.26	12
8	7288.28	711.20	-0.5	434.34	35.81	411.48	57.40	27.58	32.26	12
9	8807.20	863.60	-0.5	434.34	35.81	411.48	57.40	27.58	32.26	12
10	5687.06	558.80	-0.5	434.34	35.81	411.48	57.40	68.95	32.26	12
11	6741.67	711.20	-0.5	434.34	35.81	411.48	57.40	68.95	32.26	12
12	8037.58	863.60	-0.5	434.34	35.81	411.48	57.40	68.95	32.26	12
13	5896.10	558.80	-0.5	406.40	27.18	403.86	43.69	27.58	35.81	20
14	7342.12	711.20	-0.5	406.40	27.18	403.86	43.69	27.58	35.81	20
15	9046.97	863.60	-0.5	406.40	27.18	403.86	43.69	27.58	35.81	20
16	5516.12	558.80	-0.5	406.40	27.18	403.86	43.69	68.95	35.81	20
17	6762.75	711.20	-0.5	406.40	27.18	403.86	43.69	68.95	35.81	20
18	8168.89	863.60	-0.5	406.40	27.18	403.86	43.69	68.95	35.81	20
19	6051.80	558.80	-0.5	406.40	27.18	403.86	43.69	27.58	32.26	12
20	7408.93	711.20	-0.5	406.40	27.18	403.86	43.69	27.58	32.26	12
.	.	.	.	.	.	.	.	.	.	.
.	.	.	.	.	.	.	.	.	.	.
.	.	.	.	.	.	.	.	.	.	.
573	40227.25	863.60	1	332.74	18.03	312.42	28.19	27.58	32.26	12
574	22655.53	558.80	1	332.74	18.03	312.42	28.19	68.95	32.26	12
575	28604.72	711.20	1	332.74	18.03	312.42	28.19	68.95	32.26	12
576	34830.26	863.60	1	332.74	18.03	312.42	28.19	68.95	32.26	12

5.1 Evaluation of neural network performance

In this section, the performance of the multilayer perceptron neural network is investigated by various algorithms and it will be compared with analytical results. Regarding the algorithms used in previous researches and investigation of various algorithms in terms of suitability for this study, multilayer neural networks was performed with Levenberg-Marquardt (LM) and Bayesian Regularization (BR) algorithms in MATLAB software. First, the number of neurons and optimal network structure were investigated.

5.2 Selecting the number of hidden layer neurons

Selection of neurons has a very important impact on neural network performance. In the case of uncontrolled increase of neurons, overfitting occurs. That is, the modeled neural network offers accurate results with specific samples but by using this model in samples other than the samples used in network, we face very inaccurate results. Various methods have been proposed in order to determine the number of neurons to prevent overfitting. Some of these methods only depend on the number of inputs, and some depend on the number of inputs and outputs at the same time.

According to Kolmogorov theory the number of hidden layer neurons K must be equal to square root of multiplication of inputs and outputs.

$$K = \sqrt{M.N} \tag{3}$$

By using this formula, the number of neurons will be 19. Normally, the number of neurons is between the number of inputs and the number of outputs, and also their number is never twice more than the number of inputs. The following experimental formula is presented to find the right value.

$$K = (M + N)^{2/3} \tag{4}$$

By using this formula, the number of neurons must be 13. Also based on researches of Hush and Horne (1993) the maximum number of hidden layer neurons must be based on the following formula:

$$K \leq 2M + 1 \tag{5}$$

Therefore, the number of neurons must not exceed 21.

In this study, the number of training data is 403 (70% randomly selected from 576) for braced frames. Based on the previous values and examination of different values for the number of neurons, the number 14 had the best results.

5.3 The output results of neural network

In this section the performance of modeled neural network for the frames is investigated using LM and BR algorithms. Fig. 8 shows the performance of trained neural network using LM algorithm for the sidesway-inhibited frames. This figure has 4 diagrams including the performance of training parts, validation, testing, and total data. The linear correlation coefficient for these parts is in the range of 0.996 and 0.998. This correlation represents a very good performance of this model for determining the behavior of composite columns.

Fig. 9 presents the performance of artificial neural network with BR algorithm for sidesway-inhibited frames. Range of variation in correlation factor R is 0.997 for test and validation data and 0.998 for train data which illustrate better performance of this algorithm rather than LM algorithm.

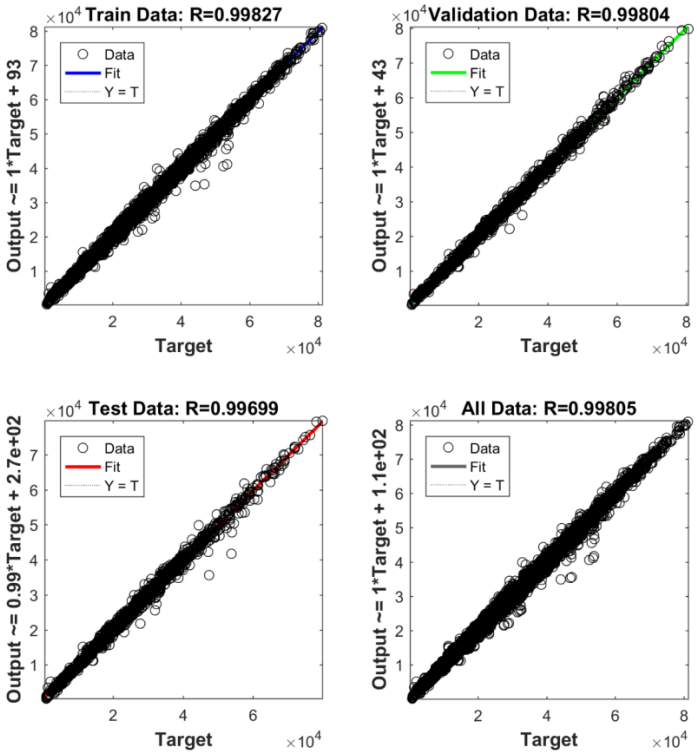

Figure 8. The results of neural network and LM algorithm on composite frames with lateral bracing

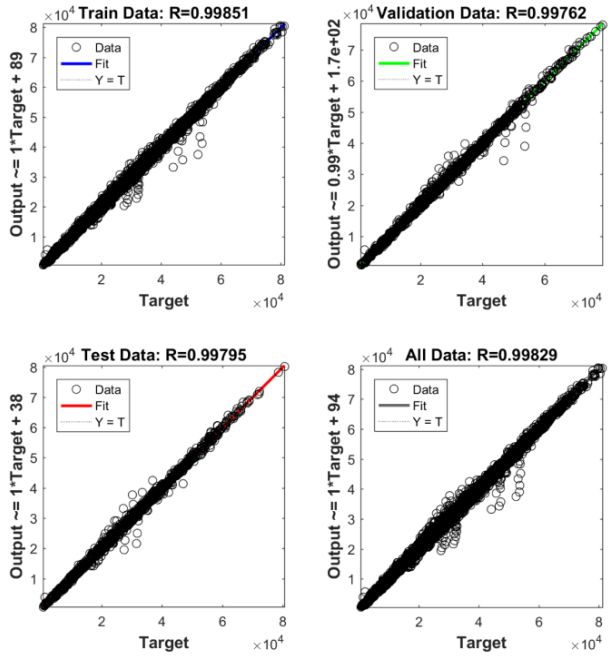

Figure 9. The results of neural network and BR algorithm on composite frames with lateral

bracing

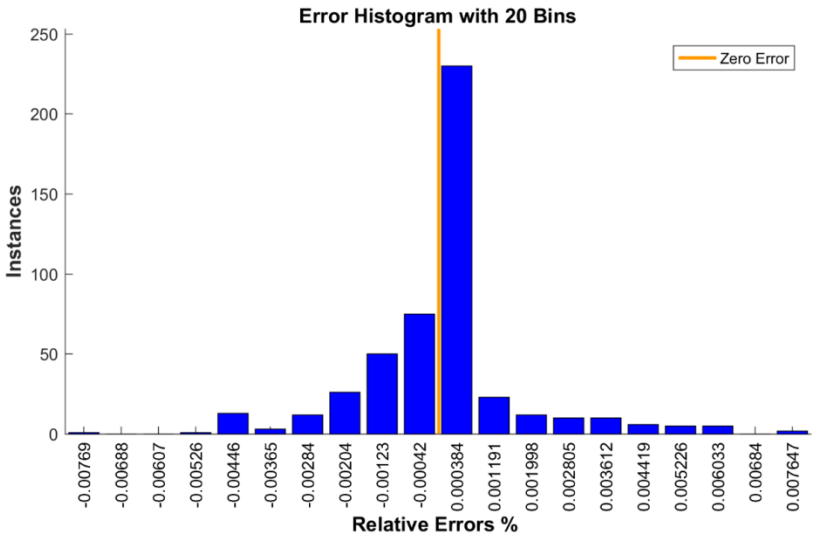

Figure 10. The histogram of relative error percentage for neural network model for frames with lateral bracing

Fig. 10 shows histogram of relative error percentage for neural network model for frames with lateral bracing. The relative error of all samples is less than 0.007%. Also error of most of samples is less than 0.001%.

5.4 Comparison of the results of analytical frames with neural network outputs

After training the neural network model for P-M_x-M_y SRC interaction curve of SRC composite columns, in order to examine the accuracy, this model was compared with the results obtained from inelastic analysis of few frames, in the range of the neural network variables. For this purpose, SRC columns with external dimensions of 610 mm in 610 mm (24 in 24 inches) and 762 mm in 762 mm (30 in 30 inches) and steel sections of W360x314 and W310x202 were considered. The specifications of sections and materials used in these samples were then given to neural network as input and estimated three-dimensional interaction curve was obtained. Also the interaction curve of each of these samples was also created by nonlinear analysis. For better comparison of two interaction curves, in axial load of 0.6Pmax two curves were cut and their M_x-M_y curves were compared in this axial load. Fig. 11 and 12 illustrates the results of sample Spec8 with neural network model of LM and BR algorithm in axial loads of $0.2P_{max}$, $0.4P_{max}$, $0.6P_{max}$ and $0.8P_{max}$ respectively. The ratio of obtained bending moment from neural network with the BR algorithm to bending moment of nonlinear analysis at 45-degree angle is shown in Table 8. These results indicate the high accuracy of neural network with BR algorithm in predicting the behavior of these columns.

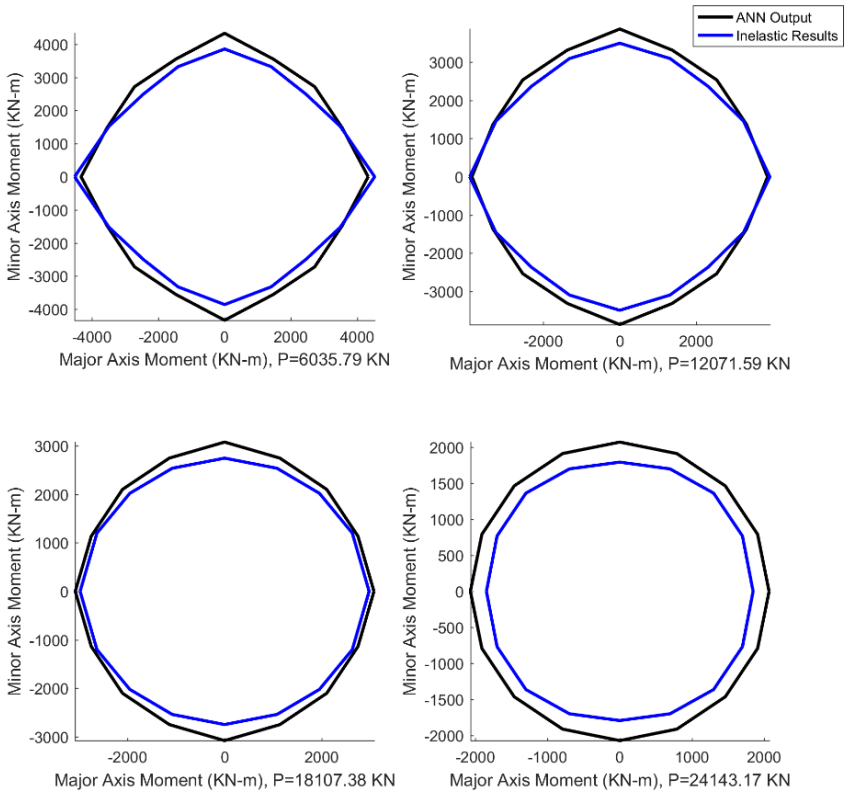

Figure 6. Comparing the results of sample Spec8 with neural network model of LM algorithm in axial loads of $0.2P_{max}$ to $0.8P_{max}$

Table 8: The ratio of estimated moments of neural network to nonlinear analysis moment

Spec.	d(mm)	t_w(mm)	b_f(m)	t_f(mm)	H(mm)	f_c(MPa)	d_b(mm)	config	L(mm)	P_{exp} (KN)	$M_{ANN}/M_{Inelastic}$ at 45°
Spec1	340.36	20.07	314.96	31.75	609.60	27.58	35.81	20	4064	15286	1.01
Spec2	398.78	24.89	401.32	39.62	762.00	27.58	35.81	20	4064	21632.18	0.94
Spec3	398.78	24.89	401.32	39.62	609.60	27.58	35.81	20	4064	18040.78	0.97
Spec4	340.36	20.07	314.96	31.75	762.00	27.58	35.81	20	4064	19013.38	1
Spec5	340.36	20.07	314.96	31.75	609.60	27.58	35.81	20	8128	12273.81	1.03
Spec6	398.78	24.89	401.32	39.62	762.00	27.58	35.81	20	8128	19150.33	0.98
Spec7	398.78	24.89	401.32	39.62	609.60	27.58	35.81	20	8128	14394.26	0.98
Spec8	340.36	20.07	314.96	31.75	762.00	27.58	35.81	20	8128	16976.95	1.01
									Mean		0.99
									Standard Deviation (SD)		0.03
									Coefficient of Variation (COV)		0.03

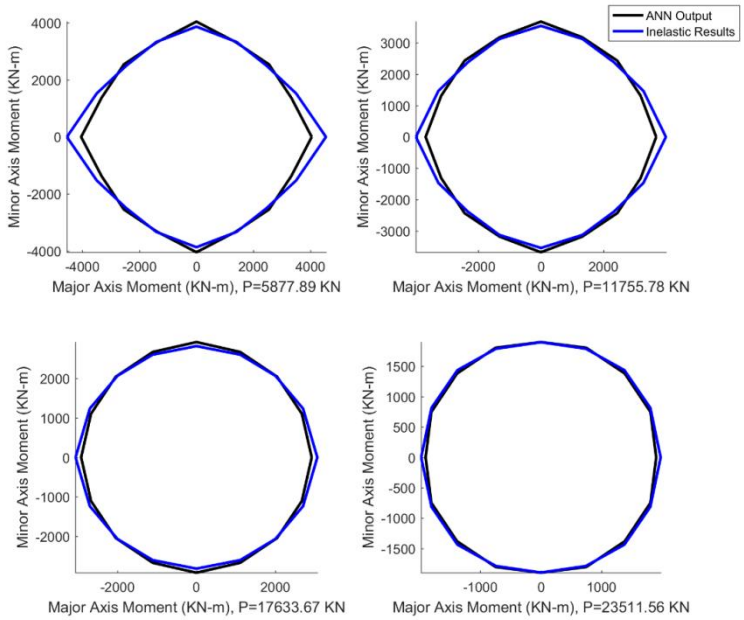

Figure 12. Comparing the results of sample Spec8 with neural network model of BR algorithm in axial loads of $0.2P_{max}$ to $0.8P_{max}$

6. CONCLUSION

In this study, a nonlinear analysis of composite beam-columns was carried out by using mixed beam-column formulation and fiber elements to make P-M_x-M_y three-dimensional interaction curves. Then, by using benchmark frames, a large set of SRC composite beam-columns with different properties was selected and their three-dimensional interaction curves were obtained. By using this data, artificial neural network was trained to estimate the complex behavior of these beam–columns. Two different algorithms for modeling of the neural network were used and the accuracy of each of them was analyzed using the analytical results in the range of neural network variables. These results indicate that the generated models can present a proper estimation of the nonlinear behavior of composite beam-columns.

REFERENCES

1. Schneider SP. Axially loaded concrete-filled steel tubes, *J Struct Eng* 1998; **124**(10): 1125-38.
2. Johansson M, Gylltoft K. Mechanical behavior of circular steel–concrete composite stub columns, *J Struct Eng* 2002; **128**(8): 1073-81.
3. Varma AH, et al. Seismic behavior and modeling of high-strength composite concrete-filled steel tube (CFT) beam–columns, *J Construct Steel Res* 2002; **58**(5): 725-58.

4. Hu H-T, et al. Nonlinear analysis of axially loaded concrete-filled tube columns with confinement effect, *J Struct Eng* 2003; **129**(10): 1322-9.
5. Hajjar JF, Gourley BC. A cyclic nonlinear model for concrete-filled tubes. I: Formulation, *J Struct Eng* 1997; **123**(6): 736-44.
6. El-Tawil S, Deierlein GG. Nonlinear analysis of mixed steel-concrete frames. I: Element formulation, *J Struct Eng* 2001; **127**(6): 647-55.
7. Inai E, et al. Behavior of concrete-filled steel tube beam columns, *J Struct Eng* 2004; **130**(2): 189-202.
8. Hajjar JF, Molodan A, Schiller PH. A distributed plasticity model for cyclic analysis of concrete-filled steel tube beam-columns and composite frames, *Eng Struct* 1998; **20**(4-6): 398-412.
9. Aval S, Saadeghvaziri M, and Golafshani A. Comprehensive composite inelastic fiber element for cyclic analysis of concrete-filled steel tube columns, *J Eng Mech* 2002; **128**(4): 428-37.
10. Tort C, Hajjar JF. Mixed finite element for three-dimensional nonlinear dynamic analysis of rectangular concrete-filled steel tube beam-columns, *J Eng Mech* 2010; **136**(11): 1329-39.
11. Denavit MD, Hajjar JF. Nonlinear seismic analysis of circular concrete-filled steel tube members and frames, *J Struct Eng* 2012; **138**(9): 1089-98.
12. Patel VI, Liang QQ, Hadi MN. Biaxially loaded high-strength concrete-filled steel tubular slender beam-columns, Part II: Parametric study, *J Construct Steel Res* 2015; **110**: 200-7.
13. Denavit MD, et al. Stability analysis and design of composite structures, *J Struct Eng* 2016; **142**(3): 04015157.
14. Virdi K, et al. Discussion. The ultimate strength of composite columns in biaxial bending, *Proceedings of the Institution of Civil Engineers* 1973; **55**(3): pp. 739-41.
15. Morino S, Matsui C, Watanabe H. Strength of biaxially loaded SRC columns, *Composite and Mixed Construction*, ASCE, 1984.
16. Munoz PR, Hsu CTT. Behavior of biaxially loaded concrete-encased composite columns, *J Struct Eng* 1997; **123**(9): 1163-71.
17. Kaveh A, Iranmanesh A. Comparative study of backpropagation and improved counterpropagation neural nets in structural analysis and optimization, *Int J Space Struct* 1998; **13**(4): 177-85.
18. Iranmanesh A, Kaveh A. Structural optimization by gradient-based neural networks, *Int J Numer Meth Eng* 1999; **46**(2): 297-311.
19. Kaveh A, Iranmanesh A. Structural optimization by neural networks, *Amirkabir J Sci Technol* 1999.
20. Ahmadi M, Naderpour H, and Kheyroddin A. Utilization of artificial neural networks to prediction of the capacity of CCFT short columns subject to short term axial load, *Arch Civil Mech Eng* 2014; **14**(3): 510-7.
21. Ahmadi M, Naderpour H, Kheyroddin A. ANN model for predicting the compressive strength of circular steel-confined concrete, *Int J Civil Eng* 2017; **15**(2): 213-21.
22. Kaveh A, Fazel-Dehkordi D, Servati H. Prediction of moment-rotation characteristic for saddle-like connections using FEM and BP neural networks, *International Conference on Engineering Computational Technology* 2000.
23. Kaveh A, Elmieh R, Servati H. Prediction of moment-rotation characteristic for semi-rigid connections using BP neural networks, 2001.
24. Afaq A, Cotsovos DM, Lagaros ND. Assessing the effect of steel fibres on the load bearing capacity of RC Beams through the use of Artificial Neural Networks, 2015.

25. Kaveh A, Servati H. Design of double layer grids using backpropagation neural networks, *Comput Struct* 2001; **79**(17): 1561-8.
26. Kaveh A, Servati H. Neural networks for the approximate analysis and design of double layer grids, *Int J Space Struct* 2002; **17**(1): 77-89.
27. Kaveh A, Raiessi Dehkordi M. Application of artificial neural networks in predicting the deformation of domes under wind load, *Int J IUST* 2007; **18**(2007): 45-53.
28. Kumar M, Yadav N. Buckling analysis of a beam–column using multilayer perceptron neural network technique, *J Franklin Institute* 2013; **350**(10): 3188-204.
29. Rofooei F, Kaveh A, Farahani F. Estimating the vulnerability of the concrete moment resisting frame structures using artificial neural networks, *Int J Optim Civil Eng* 2011; **1**(3): 433-48.
30. Kotsovou GM, Cotsovos DM, Lagaros ND. Assessment of RC exterior beam-column joints based on artificial neural networks and other methods, *Eng Struct* 2017; **144**: 1-18.
31. Sadowski L, Hoła J. Neural prediction of the pull-off adhesion of the concrete layers in floors on the basis of nondestructive tests, *Procedia Eng* 2013; **57**: 986-95.
32. Denavit MD, Hajjar JF, Characterization of behavior of steel-concrete composite members and frames with applications for design, University of Illinois at Urbana-Champaign, 2014.
33. ANSI B. AISC 360-16-specification for structural steel buildings, Chicago AISC, 2016.
34. ACI, Building Code Requirements for Structural Concrete and Commentary (ACI 318-14). 1 ed, American Concrete Institute, 2015.
35. Chang G, Mander JB. Seismic energy based fatigue damage analysis of bridge columns: part 1-evaluation of seismic capacity, 1994.
36. Popovics S. A numerical approach to the complete stress-strain curve of concrete, *Cement Concrete Res* 1973; **3**(5): 583-99.
37. Mander JB, Priestley MJ, Park R. Theoretical stress-strain model for confined concrete, *J Struct Eng* 1988; **114**(8): 1804-26.
38. Alemdar BN, White DW. Displacement, flexibility, and mixed beam–column finite element formulations for distributed plasticity analysis, *J Struct Eng* 2005; **131**(12): 1811-9.
39. De Souza RM, Force-based finite element for large displacement inelastic analysis of frames, University of California, Berkeley California, 2000.
40. Nukala PKV, White DW. A mixed finite element for three-dimensional nonlinear analysis of steel frames, *Comput Meth Appl Mech Eng* 2004; **193**(23): 2507-45.
41. Kanchanalai T. The design and behavior of beam-columns in unbraced steel frames, AISI Project No. 189, Report, 1977.
42. Surovek-Maleck AE, White DW. Alternative approaches for elastic analysis and design of steel frames. I: Overview, *J Struct Eng* 2004; **130**(8): 1186-96.
43. Surovek-Maleck AE, White DW. Alternative approaches for elastic analysis and design of steel frames. II: Verification studies, *J Struct Eng* 2004; **130**(8): 1197-205.